

491

BNL-12757

Conf-680811--8
10/21/68

MASTER

LEGAL NOTICE

This report was prepared as an account of Government sponsored work. Neither the United States, nor the Commission, nor any person acting on behalf of the Commission:

A. Makes any warranty or representation, expressed or implied, with respect to the accuracy, completeness, or usefulness of the information contained in this report, or that the use of any information, apparatus, method, or process disclosed in this report may not infringe privately owned rights; or

B. Assumes any liabilities with respect to the use of, or for damages resulting from the use of any information, apparatus, method, or process disclosed in this report.

As used in the above, "person acting on behalf of the Commission" includes any employee or contractor of the Commission, or employee of such contractor, to the extent that such employee or contractor of the Commission, or employee of such contractor prepares, disseminates, or provides access to, any information pursuant to his employment or contract with the Commission, or his employment with such contractor.

PuO₂-UO₂-Na Aerosols Produced

By Vaporization of Fast Reactor Core Materials* **

F. L. Horn and A. W. Castleman, Jr.

Brookhaven National Laboratory, Upton, New York, U.S.A.

Introduction

The prospect that the continued development of fast reactors fueled with plutonium will result in an abundance of these reactor types requires careful consideration of their safety aspects. Numerous safeguards engineered into their construction and operation should cope with nearly all foreseeable accident conditions of the first and second level.

When consideration is given to the third level of reactor safety, i.e., to the highly unlikely occurrence of a simultaneous failure of all protective systems at the time of a reactor accident, it must be assumed that the coolant is expelled from the core and gross melting and vaporization of the fuel occurs.

In the case of sodium cooled fast breeder reactors fueled with plutonium-uranium oxide, the hypothetical accident predicates gross melting of the fuel, compaction of the core producing a prompt critical reactor period, followed by vaporization of fuel and coolant to the containment vessel. The resultant vapor will condense into an aerosol composed of PuO₂ and UO₂ mixed with Na. The time dependent behavior of the aerosol with respect to coagulation, settling, wall plating, particle size distribution, and particle density is of interest to persons concerned with the possible effect of such an accident on the rate of leakage from the reactor containment and its impact on siting considerations and salvage operations.

*This research was performed under the auspices of the USAEC.

**This paper was presented at the Symposium on Operating and Developmental Experience in the Treatment of Airborne Radio-Active Wastes, New York, Aug. 26-30, 1968. Sponsored by IAEA.

DISCLAIMER

This report was prepared as an account of work sponsored by an agency of the United States Government. Neither the United States Government nor any agency thereof, nor any of their employees, makes any warranty, express or implied, or assumes any legal liability or responsibility for the accuracy, completeness, or usefulness of any information, apparatus, product, or process disclosed, or represents that its use would not infringe privately owned rights. Reference herein to any specific commercial product, process, or service by trade name, trademark, manufacturer, or otherwise does not necessarily constitute or imply its endorsement, recommendation, or favoring by the United States Government or any agency thereof. The views and opinions of authors expressed herein do not necessarily state or reflect those of the United States Government or any agency thereof.

DISCLAIMER

Portions of this document may be illegible in electronic image products. Images are produced from the best available original document.

The extremely low human tolerance for plutonium is for many situations the determining factor over the radiation effects of fission products^[1]; therefore, fission products have been excluded from the initial phases of this study.

Experimental Apparatus and Procedure

All of the experiments were carried out using a resistance heater to rapidly vaporize the materials into a flowing gas stream. The heater assembly consisted of a high resistance ribbon filament suspended between two water-cooled copper blocks. Utilizing a power-stat and a 12-volt a.c. power supply, a current of 500 amperes was passed through the filament on which the sample was placed. A temperature of 3000°C could be attained in 3 to 5 seconds. The compound PuO₂ melts at 2390°C, while UO₂ melts at a somewhat higher temperature of 2840°C.^[2] Therefore, the PuO₂ vaporization experiments were carried out at \approx 2700°C, while a temperature near 3000°C was required to vaporize equal quantities of UO₂ and PuO₂-UO₂ mixtures in similar periods of time. The vaporization usually required from 30 to 45 seconds to be completed, depending upon the sample size. In some of the initial PuO₂ experiments, the vaporization was done in a small chamber and the aerosol transported by a gas stream through a duct to the settling chamber. In these experiments, the gas flow was maintained at \approx 50 cc/min during vaporization and was terminated after the visible aerosol fume was carried into the settling chamber. The fuel vaporization apparatus was installed directly on the floor of the main settling chamber for all runs with UO₂ and the latter ones with PuO₂.

Although experiments were carried out in which the sodium and fuel oxide were both placed on the heater filament, it was generally more satisfactory to vaporize the sodium with a separate resistance heater located adjacent to the main filament. Because of the widely differing vapor pressures of PuO₂ and sodium, the sodium could be readily vaporized at temperatures below 900°C, considerably lower than those required to vaporize the fuel. Experiments were done in atmospheres of argon, nitrogen, and air with relative humidities as high as 70%. Numerous preliminary screening experiments showed tantalum carbide to be the best filament material, producing no detectable aerosol in all "blank" experiments except in those of high moisture levels.

Several settling chambers were employed during the course of these experiments. Due to the health hazard associated with plutonium, all components of the apparatus were enclosed within a glove box. This severely restricted the maximum size of the settling chamber which could be employed in these studies and necessitated the use of chambers which could be readily removed

from the glove box and replaced. Therefore, the larger chambers of 1 cubic meter and 0.75 cubic meter in size were constructed of a specially treated polyethylene material, 0.006 gauge Antistatic Polyethylene Film. The height of both of these enclosures is one meter. A Lucite settling chamber, 0.40 meters in height, was also employed. The surface-to-volume ratio of each of these enclosures was 6.0, 6.6, and 30 m^{-1} , respectively.

Since the primary objective of these studies was an investigation of the quantity of plutonium oxide remaining airborne, emphasis was placed on sampling the airborne concentration and size distribution as a function of time. This was accomplished using thermal precipitators. Their principle of operation is based on the thermophoresis effect.^[3] Briefly, a gas sample is withdrawn from the aerosol enclosure at the rate of $\approx 7 \text{ cc/min}$ for several minutes. The gas stream containing the aerosol particles is drawn past a hot wire. The aerosol particles deposit on electron microscope grids located in the center of the plugs inserted in each precipitator. The carbon-coated microscope grids are attached to the face of each plug. These are then inserted into the hole adjacent to the wire for each sampling operation. The plugs are removed after the sample is taken and the grids are mounted in a Phillips EM 100B electron microscope for examination.

Pictures are taken of the representative particles deposited on the carbon coating. The count mean diameter of the aerosol particles is determined using a Zeiss TGZ3 particle-size counter.

A number of calibration experiments showed the over-all particle collection efficiency of these precipitators to be better than 95% for the particle size ranges of interest in this study. The plutonium mass concentration data was obtained by alpha-counting of the plutonium deposited on the grids. In addition, plate-out sampling of the floor and walls of the enclosure was done in some experiments.

Results

The vapor of both PuO_2 and UO_2 condenses into cubic crystals that form into long twisting chains characteristic of metal oxides. See Figures 1 and 2. The experimental results showed that the nature of PuO_2 vaporized into nitrogen, argon, and dry air was essentially the same. In each case the individual nucleated particles rapidly agglomerated into branched chains typified by those shown in Figures 3 to 5. Figure 3 is an enlargement of one opening of an electron microscope grid and shows the typical flocculent appearance of the particles and their widely varying size distribution. Figure 4, an

enlargement of several of the agglomerates, shows the cubic structure of the individual particles making up the agglomerate with some sodium present. These structures are typical of oxide particles nucleating from a vapor phase.

Experiments in which sampling time and gas flow rate through the thermal precipitator were varied, clearly showed that these agglomerates accurately represent the characteristics of the airborne material and are not built up on the collection surfaces. Unlike cascade impactor sampling, the thermal precipitators do not have the tendency to destroy the original gas phase agglomerate structures. Figure 5 reveals the three-dimensional nature of the particles. This photograph is a shadow-graph of a PuO_2 aerosol deposit which was made by vaporizing chromium oxide onto a collection grid tilted at an angle of 30° to the vaporizing source beam. The light areas are due to a lack of deposited chromium oxide caused by the vertical structure of the particle protruding between the vapor path and the inclined grid surface.

Visually, deposits of PuO_2 and UO_2 aerosols appear to be similar as seen in Figures 6a and 6b. It is evident that both UO_2 and PuO_2 aerosols are composed of chainlike agglomerates made up of small cube-like particles. The UO_2 agglomerates are usually somewhat larger in physical size than the corresponding PuO_2 ones, resulting in a more rapid settling of the pure UO_2 as well as mixed PuO_2 - UO_2 .

A plot of the change in airborne plutonium mass concentration as a function of time is shown in Figures 7 and 8 for the 17.4 liter and 0.75 cubic meter chambers, respectively. Invariably, the aerosol mass concentration initially drops very rapidly, leveling off to a much slower rate of decrease after the initial period. Usually, several days of settling time are required before the airborne plutonium oxide concentration drops below 10^{-7} g/m³, the limit of detection. The behavior of pure PuO_2 shown on Figure 8 indicates the concentration drops through three orders of magnitude in two days with a leveling off at 10^{-5} g Pu/m^3 which is four times the background alpha count. This aerosol was generated directly in the chamber. The concentration reaches zero or background count after one week's time in the three-quarter m³ chamber.

The aerosol particles within the agglomerates, as well as the size distribution of the agglomerates themselves, are well represented by a log-normal distribution. That is, the number of particles per unit volume of diameter d , n_d , are adequately represented by the relationship:

$$n_d = \frac{N}{\log \sigma_g \sqrt{2\pi}} \exp \left[\frac{-(\log d - \log d_g)^2}{2 \log^2 \sigma_g} \right],$$

where N is the total number of particles per unit volume, d_g is the count mean diameter (CMD) and σ_g is the standard deviation. The individual particles of an agglomerate range in size from 30 \AA to 0.04μ and have a standard deviation around 2.0.

The count mean diameters of the PuO_2 agglomerates were usually found to be within the range 0.15 to 0.20μ with σ_g ranging from 1.7 to 2.0. Typical plots of the log-normal distribution of an aerosol sampled at 10 minutes, one hour, and seven hours are shown in Figures 9a, 9b, and 9c, respectively. The particle sizes for Figure 8 are initially 0.128μ to 0.178 microns after 27 hr. The geometric standard deviation went from 2.0 to 2.8 at 27 hr.

To investigate the nature of mixed PuO_2 -Na aerosols, an aerosol with a Na/ PuO_2 ratio of 12.5:1 was generated in the 0.75 cubic meter chamber containing dry nitrogen gas. The aerosol was found to consist largely of composite Na- PuO_2 aggregates after one hour of settling. After 48 hours, no particles were observed in the samples, and the alpha count had dropped to about four times background. These results are similar to the ones obtained with a Na/ PuO_2 ratio of 75:1. The variation of count mean diameter with time for this experiment is shown in Figure 10. The CMD is seen to reach a maximum between 0.6 and 0.8 microns in one to two hours of settling time. Subsequently, the larger particles settle leaving airborne ones with a CMD of around 0.23 microns. A plot of the PuO_2 mass concentration as a function of time is shown in Figure 11. The PuO_2 mass concentration was found to decrease by three orders of magnitude in 24 hr from a measured value of 10 mg/m^3 sampled at 5 min. The nominal initial PuO_2 mass concentration was 56 mg/m^3 , based on the quantity of PuO_2 vaporized into the chamber.

A picture of the PuO_2 -Na aerosol taken at a magnification of 224,000 clearly shows the cubic structure of the PuO_2 crystals as seen in Figure 12. A coating of lighter density sodium or sodium hydroxide along with larger sodium spheres is also visible. The PuO_2 cubes range in size from $<50 \text{ \AA}$ to about 0.1 microns, and are generally smaller in size than the UO_2 cubes shown in earlier reports. The aggregates of PuO_2 are composed of many of these small cubic particles.

The possibility of aerosol resuspension as a result of the agitated movement of the settling chamber walls was

investigated. The chamber was sampled prior to and after the chamber was collapsed from the sides and bottom following a plutonium aerosol run. No particles were found on the thermal precipitator sample grids before or after the agitation, indicating little or no resuspension due to movement of the chamber sides. Therefore, the persistent nature of the airborne plutonium concentration is evidently associated with the physical characteristics of the aerosol.

A UO_2 aerosol was generated in the 0.81-m^3 chamber containing nitrogen gas with a relative humidity of 70%. The aerosol had an initial mass concentration of 30 mg/m^3 and a CMD of 0.13 microns, with a σ_g of 2.4. A plot of the CMD measured over a period of two days is shown in Figure 13. The CMD peaked at five hours, reaching a maximum value of 0.365 microns and leveling off to 0.088 microns at 52 hours. The nearly spherical agglomerates typical of high humidity are shown in Figure 14. This aerosol sample has a σ_g of 2.49. These data are similar to those obtained in the Na-UO_2 experiment at 27% R.H. In the earlier Na-UO_2 experiment, the particle size reached a peak value of 0.390 microns at 5 hours.

A log-normal size distribution is observed in nearly all runs as shown in Fig. 15 with pure UO_2 at 70% humidity at 5 hr 18 min; however, after 28 hr 18 min, an anomaly is found (see Figure 16). There is a break in the curve below the 50% point, the sigma increases to 3.47. This was also observed in a Na-UO_2 run at 70% humidity below the 20% point when additional high magnification photographs of the smaller particles were analyzed (see Figure 17a and 17b). This size distribution is not produced by separate Na and UO_2 particles but by combined Na-UO_2 particles as shown in Figure 18. The break is at about 0.3 microns and continues below 0.1 micron at which point the curve resumes its original slope. Less than 2% of the particles are below 0.05 microns. It is possible that with high humidity chemical reactions occur and spherical agglomeration with moisture absorption lead to a particle size distribution that is not log-normal.

Discussion

It is a well-known fact that high number density aerosols rapidly coagulate. Most experimental evidence indicates that coagulation results in nearly every collision. Consequently, the reduction in airborne plutonium concentration is mainly due to settling, while plateout on walls generally accounts for only 10 to 15% of the total material in our experiments. Airborne particles are known to settle according to Stokes equation for Reynolds numbers below 0.1. The Stokes velocity is given by the equation:

$$v_s = \frac{1}{18} \frac{g \rho d^2}{\eta}$$

where d is the diameter of the particle, ρ its effective density, g the acceleration due to gravity, and η the viscosity of the gaseous medium in which settling is occurring.

Following the work of others^[9,10] a computer program was developed to solve the equations expressing the simultaneous agglomeration and Stokes settling of an aerosol. Using the experimental data on the particle size distribution and number density of some PuO_2 aerosols, agglomeration coefficients were evaluated. Values ranged from 3×10^{-9} to $9 \times 10^{-10} \text{ cm}^3/\text{sec}$. For the particle radius, r_g , dependence versus time, the computer predicted trend was in general qualitative agreement with the experimental data. In addition, the time dependence of the total airborne mass concentration was evaluated by integrating the product of the number density, the individual particle volumes and the particle density over all values of the particle radii. The calculated mass concentration behavior with time did not quantitatively agree with the leveling off observed experimentally, indicating that the particle density varies with time.

Due to the relatively large different time scales in which the two processes operate, it is possible to use simplified equations in a semiquantitative manner. That is, initially agglomeration is very rapid while settling is relatively unimportant; for intermediate times of several minutes to several hours, settling is the dominant process while relatively little agglomeration takes place.

Sinclair^[5] has developed an approximate solution to an equation expressing the time dependence of the airborne mass concentration accounting for the settling of heterogeneous stirred aerosols.

$$-\frac{d}{dt} \ln M_t = 3.0 \times 10^5 \frac{\rho d_8^2}{h}, \text{ (where } (v_s t)/h \ll 1 \text{)}.$$

In this relationship, h is the height of the enclosure in centimeters, ρ the particle density, and d_8^2 is given by the equation

$$\log d_8^2 = 2 \log d_g + 18.424 \log^2 \sigma_g.$$

The use of the diameter d_g , in conjunction with Stokes law, adequately accounts for the distribution of particle sizes. The use of the mass mean or count mean diameter is not appropriate. Integration of $(d \ln M_t)/dt$ yields an equation for the fraction, f , of an aerosol remaining airborne as a function of time. Therefore,

$$f = \exp(-3.0 \times 10^5 \frac{\rho d_8^2}{h} t) .$$

CGS units are to be employed here. Consequently, the settling behavior of an aerosol can be determined from the product ρd_8^2 .

In our experiments, the initial behavior of the pure PuO_2 and the mixed $\text{PuO}_2\text{-UO}_2$ aerosol is in good agreement with the approximate theory. Figure 19 shows that all of the PuO_2 data, within experimental scatter, can be represented by a single semilog plot of the fraction of PuO_2 remaining airborne as a function of t/h . The deviation from a straight line after a decrease of approximately one order of magnitude is undoubtedly due to a decrease in the product ρd_8^2 with time. Although in theory the particles are growing with time, they are forming chain-like "fluffy" agglomerates whose density is much less than the theoretical (11.46 g/cm^3). The particles are likely to be of theoretical density immediately following nucleation. Particle densities ranging from 4 g/cm^3 to $<1/2 \text{ g/cm}^3$ were experimentally observed after several hours of agglomeration.

Our preliminary work indicates that the time dependence of UO_2 and mixed $\text{PuO}_2\text{-UO}_2$ aerosol mass concentrations is somewhat different from that of pure PuO_2 . This difference is shown in Figure 19 for the case of a 20 wt % PuO_2 -80 wt % UO_2 aerosol. The UO_2 and $\text{PuO}_2\text{-UO}_2$ aerosols settle more rapidly, probably due to a larger over-all ρd_8^2 . It is not too surprising to expect UO_2 and PuO_2 aerosols to differ somewhat in behavior since the vapor pressure relationships for these two oxides are considerably different, and they vaporize by different processes.^[6,7,8]

The fraction remaining airborne shown on Figure 19 indicates the effect of mass concentration on settling rate. At 0.050 g Pu/m^3 the fraction decreases one order of magnitude before leveling off. At 2.0 g Pu/m^3 the fraction decreases two orders of magnitude; however, the initial ρd^2 line remains constant at 0.458×10^{-6} . Therefore, the product of the initial densities and diameters are equal. The lower mass concentration gives smaller particle sizes after several hours by a factor of two and the sigma increases to 2.8. No peak in CMD is observed as it was in the Na-PuO_2 run (Figure 10). It is evident that the Na contributes to the peak at 0.78 microns, while in PuO_2 alone, the range of values is 0.128 to 0.22 at the end of the run. A slight peak at 0.275μ is observed at three hours.

A conservative estimate of the product ρd_8^2 can be obtained from the slope of the dotted straight line shown in Figure 19. This value should be adequate for estimating the first one to

two orders of magnitude drop in concentration. It is worthwhile noting that the product of the theoretical density and d_g^2 calculated from experimental d_g (CMD) and σ_g values is in good agreement with that obtained from the figure. Obviously, whenever possible, it is preferable to use the product ρd_g^2 deduced from the time dependence of the airborne mass concentration. Since this value is based on the aerodynamic character of the particles, no correction for their nonsphericity is needed.

The presence of sodium has some effect on the PuO_2 aerosol mass concentration behavior as seen in Figure 20. For sodium to PuO_2 ratios of 1, the long-time behavior of the aerosol is very much like that without sodium. However, with larger sodium-to- PuO_2 ratios, the experimental results indicate that the aerosol remains airborne for a much longer period of time. This observation is not unexpected. Since the densities of both sodium and its oxide are quite low compared with PuO_2 , the composite agglomerates, although larger in size, have a smaller density than the agglomerates of pure aerosols. This leads to a smaller value of ρd_g^2 and a more persistent aerosol.

At this time, we recommend the use of the following equation for making conservative estimates of the fractional decrease in aerosol concentration with time. In the absence of large excess of airborne sodium,

$$f = \exp \left(\frac{-1.37 \times 10^{-3}}{h} t \right).$$

Where large quantities of sodium (or its oxide) are vaporized together with PuO_2 , this relationship may be a valid conservative estimate for very short times. In this equation, h is the height of the reactor vessel in meters and t is time in seconds.

Acknowledgments

The authors acknowledge useful discussions with Ignatius Tang during the preparation of this paper, and thank H. Berry and C. Wawrzusin of the Applied Mathematics Department of Brookhaven National Laboratory for programming the equations governing the aerosol behavior. The invaluable assistance of D. Wales and C. Brewster in performing many of the experiments and the electron microscope work of J. Kelsch is also acknowledged.

REFERENCES

- [1] HÄFELE, W., HELLER, F., SCHIKARSKI, W. The principle of double containment and the behavior of aerosols in its relation to the safety of reactors with a high plutonium inventory, KFK 669 EUR 3702 e, October 1967.
- [2] LYON, W. L., BAILEY, W. E., The solid liquid phase diagram for the UO_2 - PuO_2 system, AEC R&D REP. #GEAP-4878, Dec. 1965.
- [3] CAWOOD, W., Trans. Faraday Soc. 32 (1963) 1068.
- [4] FUCHS, N. A., The Mechanics of Aerosols, (Translated by R. E. Faisley and Marina Fuchs). Pergamon Press (1964).
- [5] SINCLAIR, DAVID, Ch. 5, "Handbook on Aerosols," U.S. Office of Scientific R&D, Washington, D.C. (1950).
- [6] DeMARIA, G., BURNS, R. P., DROWART, J., INGHRAM, M.G., J. Chem Phys. 32 (1960) 1373.
- [7] PARDUE, W. M., KELLER, D. L., J. Am Ceram. Soc. 47 (1964) 610.
- [8] ANL-7375. Chemical Engineering Division Semiannual Report. January-June 1967, pp. 95-102.
- [9] Zebel, G., Z. Kolloid, 156, 102 (1958).
- [10] SPIEGLER, P., MORGAN, J. G., GREENFIELD, M.A., KOONTZ, R.L., "Characterization of aerosols produced by sodium fires," Vol. I. Solutions of a General Equation for the Coagulation of Heterogeneous Aerosols, NAA-SR-11997, Vol. I, (1967).

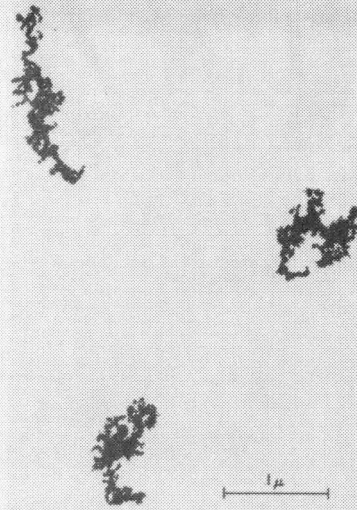


FIG.1

Typical PuO_2 chain agglomerates

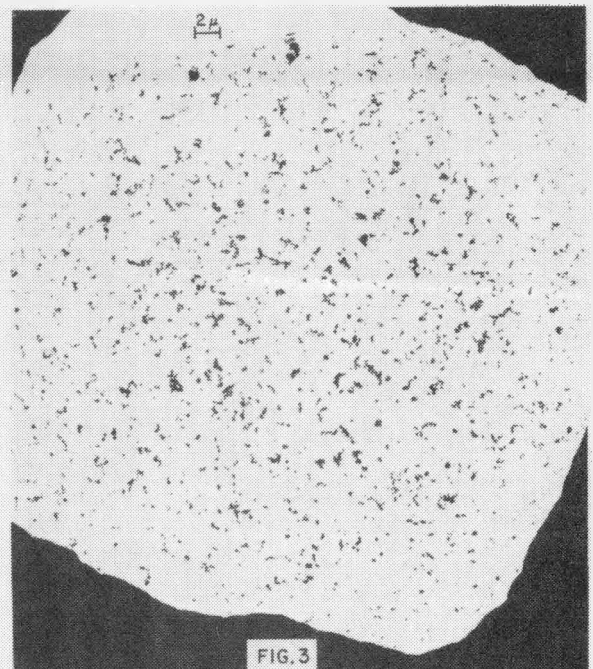


FIG.3

Electron microscope grid opening with particles of PuO_2 deposited on carbon coating showing wide size variations

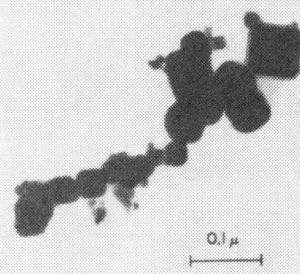


FIG.2

Cubic-shaped particles of PuO_2

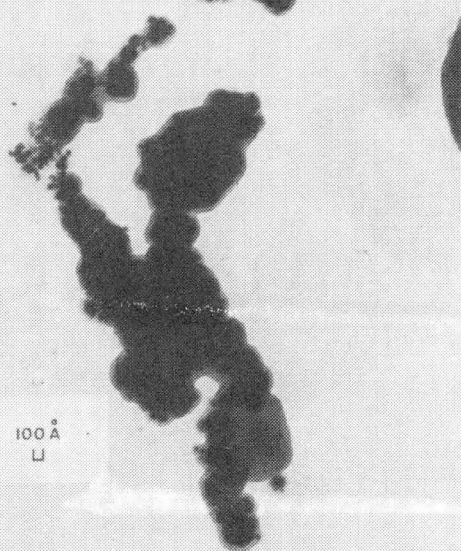


FIG.4

Cubic-shaped PuO_2 particles from $>50\text{\AA}$ to 0.1 micron in size with light colored Na coating

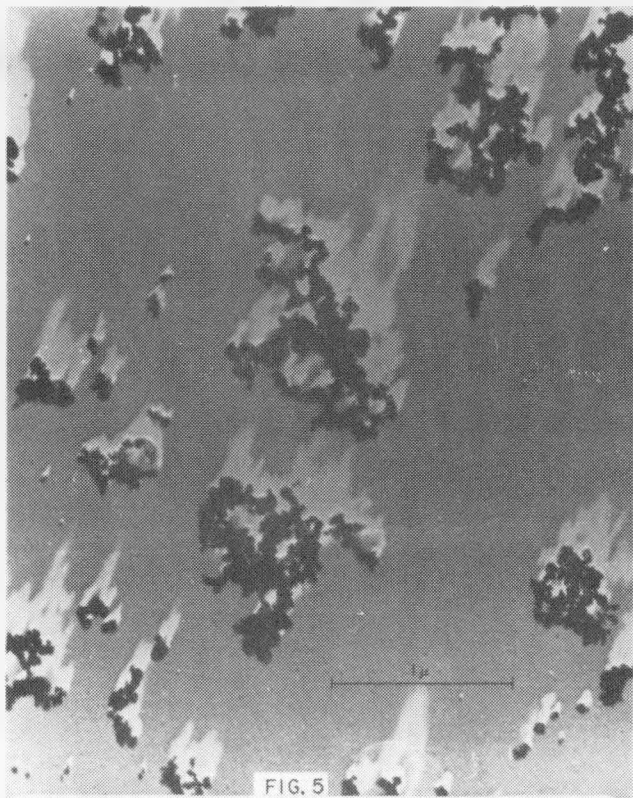


FIG. 5

Shadow-graph of PuO₂ agglomerates showing their three-dimensional nature

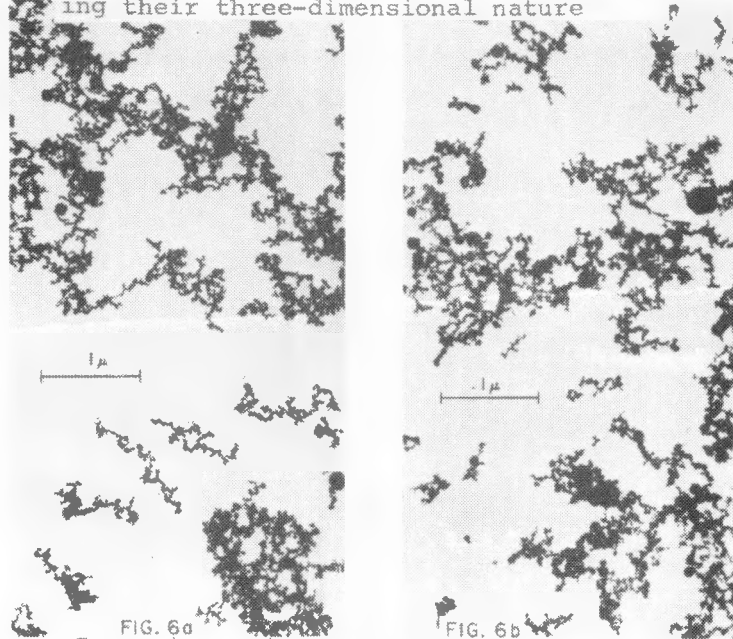
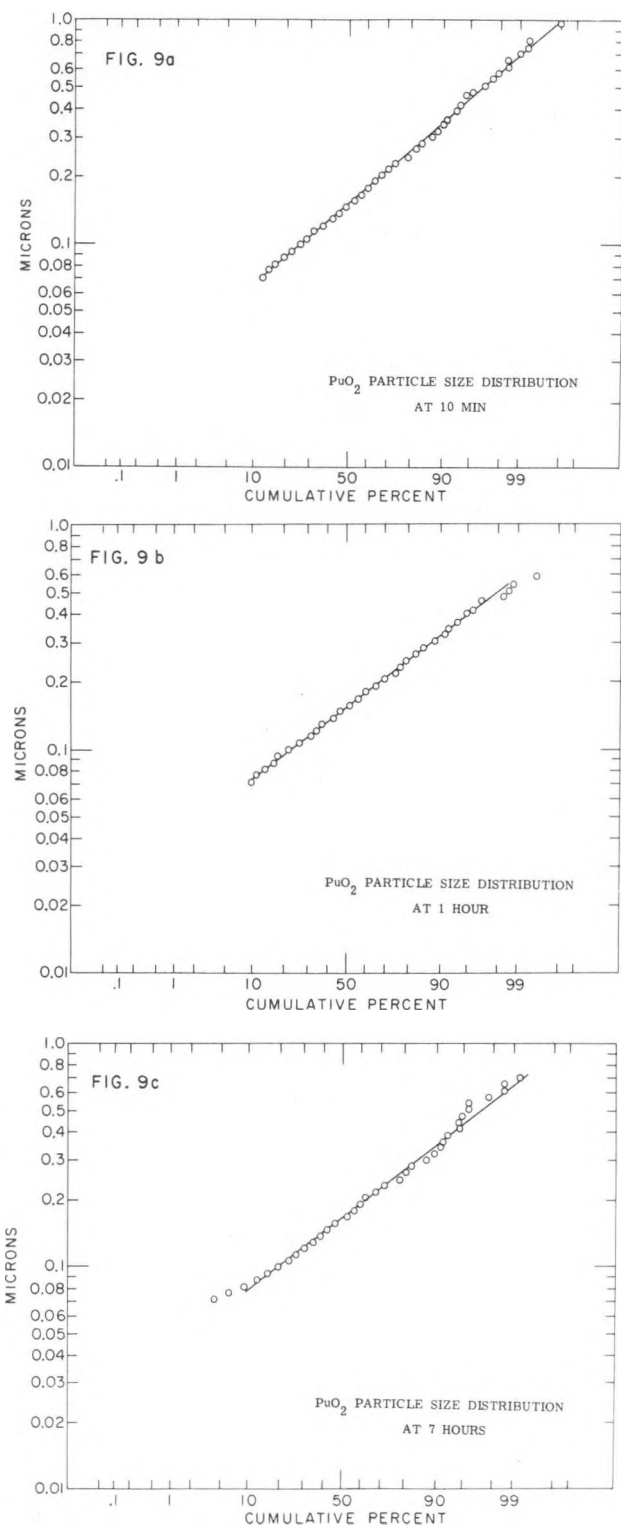
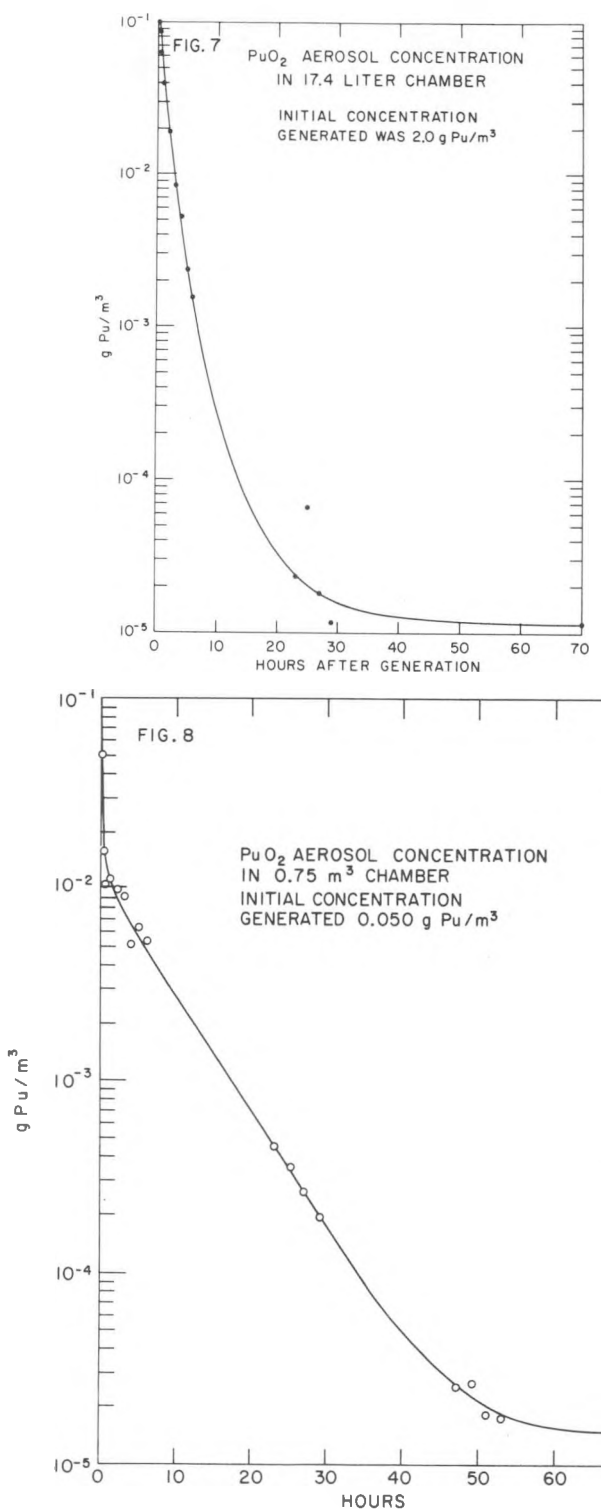


FIG. 6a
Comparison of UO₂ and PuO₂ agglomerates,
respectively, indicating similarity

FIG. 6b



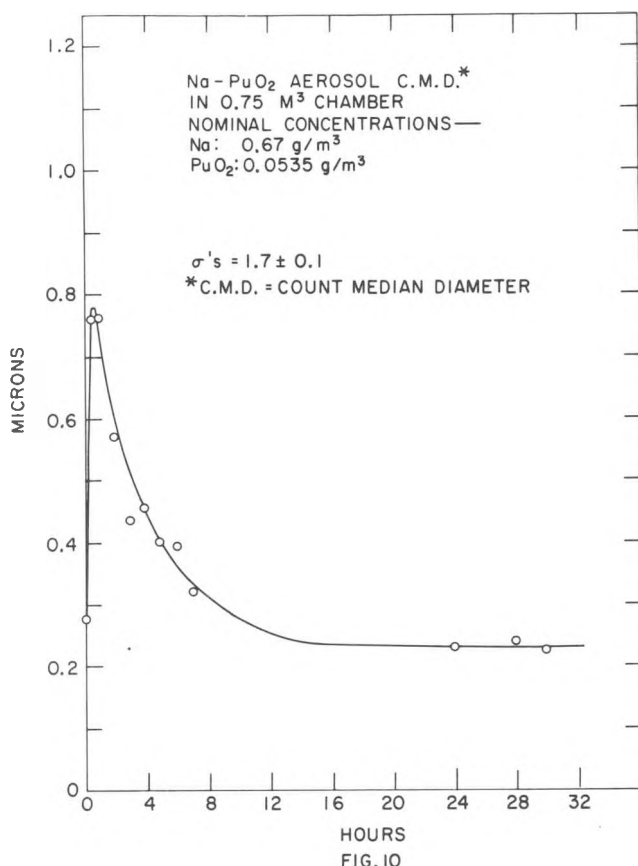


FIG. 10

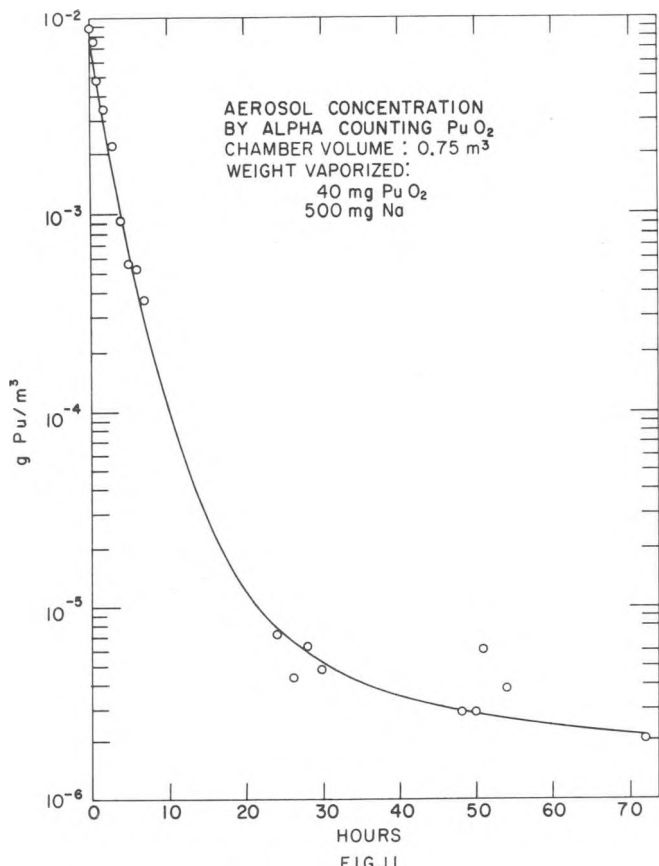


FIG. 11

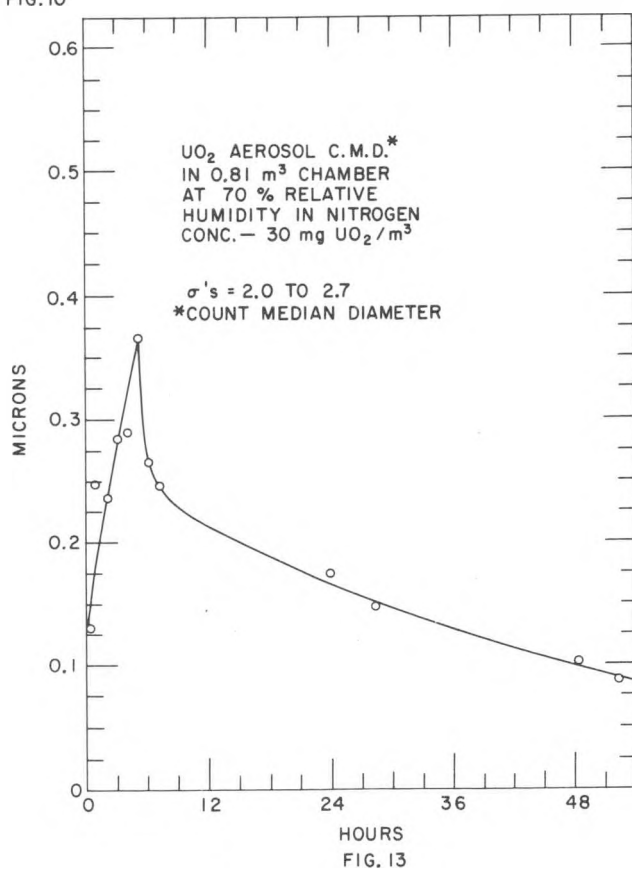


FIG. 13

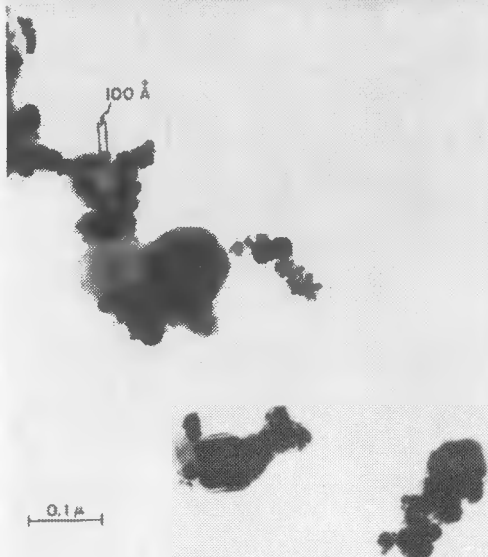


FIG. 12
Cubic PuO_2 aerosol particles
with NaOH spheres

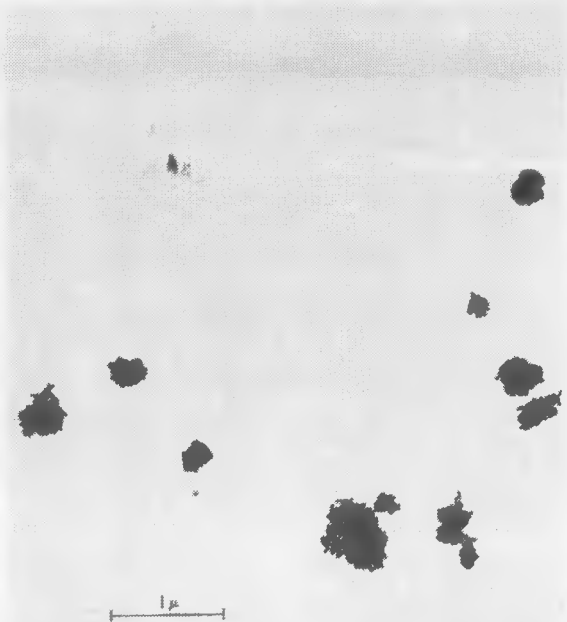
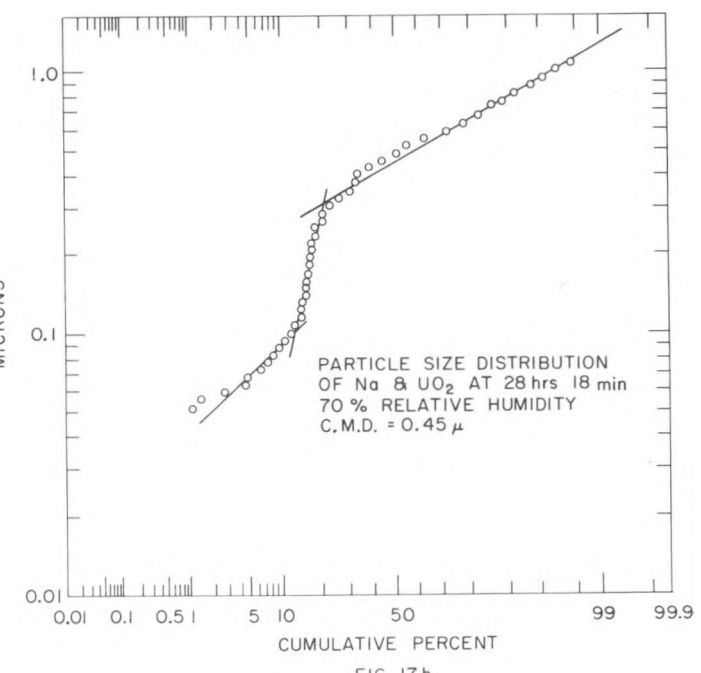
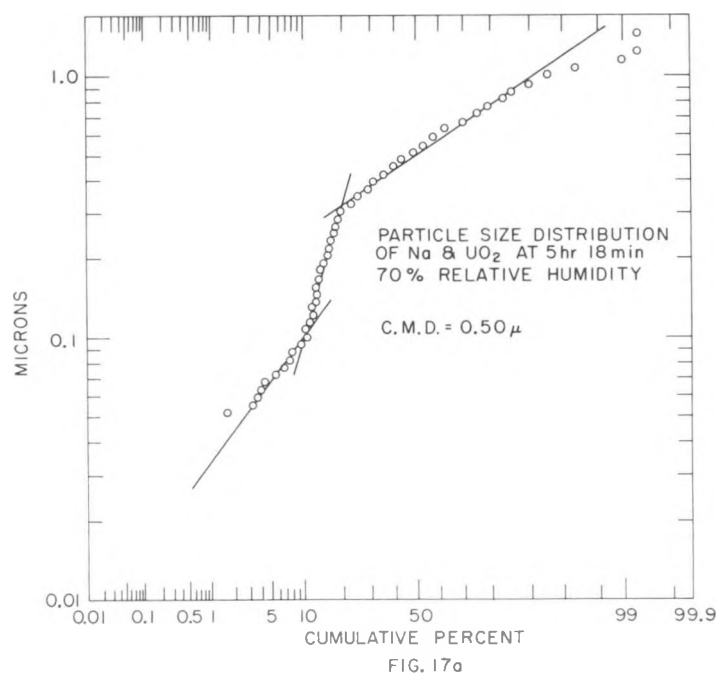
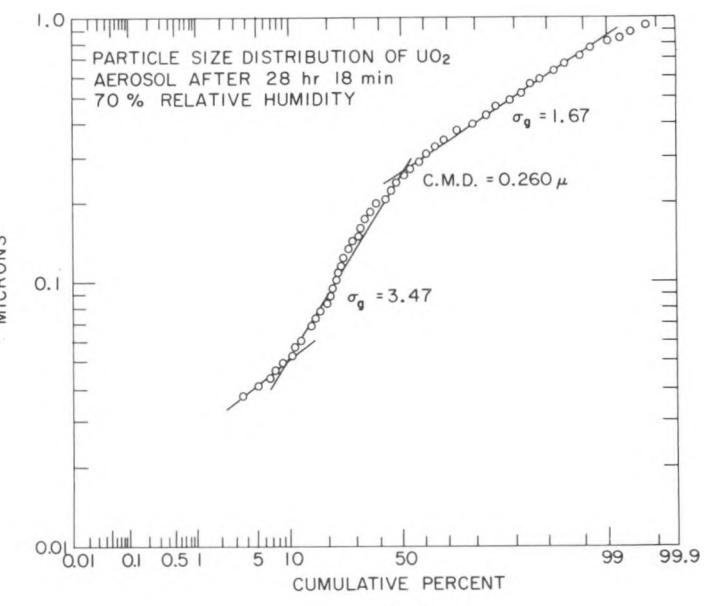
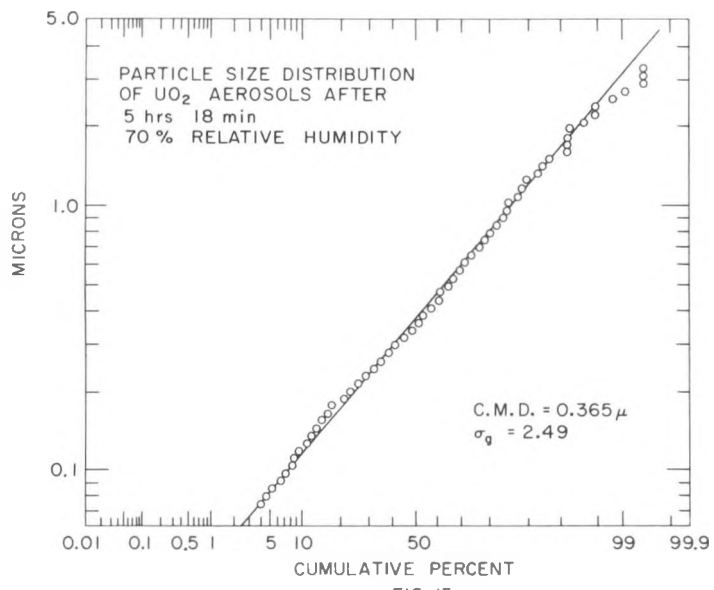


FIG. 14
Typical spherical UO_2 agglomerates in 70% relative humidity



FIG. 18
Combined Na-UO_2 particles produced
in 70% relative humidity



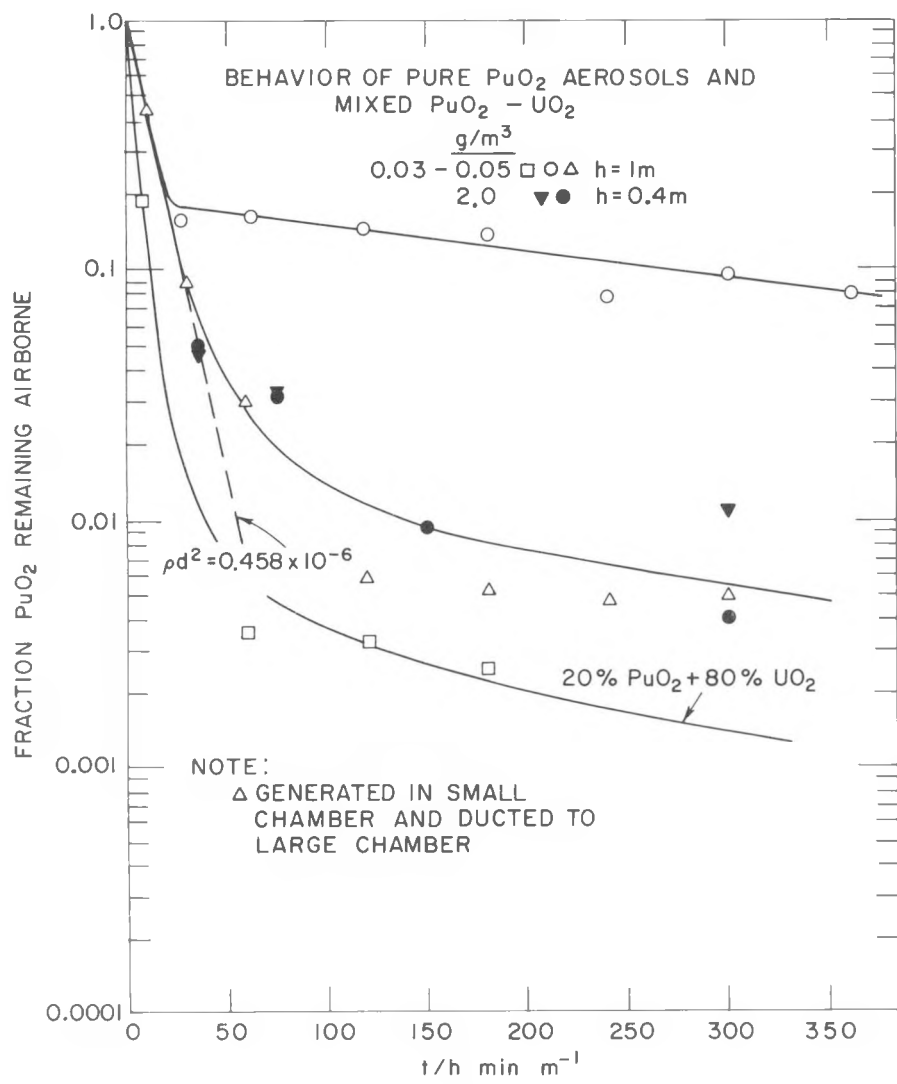


FIG. 19

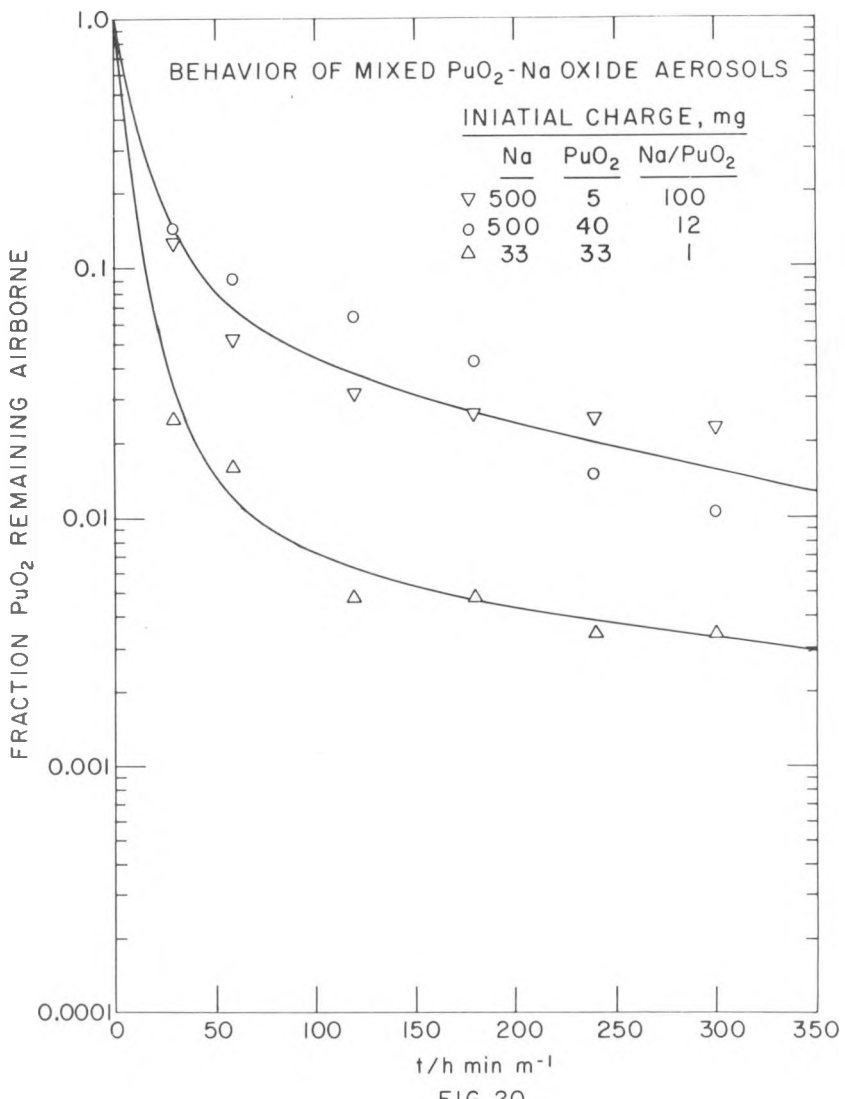


FIG. 20

List of Figures

Figure 1 Typical PuO_2 chain agglomerates.

Figure 2 Cubic-shaped particles of UO_2 .

Figure 3 Electron microscope grid opening with particles of PuO_2 deposited on carbon coating showing wide size variation.

Figure 4 Cubic-shaped PuO_2 particles from 50\AA to 0.1 micron in size with light colored Na coating.

Figure 5 Shadow-graph of PuO_2 agglomerates showing their three-dimensional nature.

Figure 6a and 6b Comparison of UO_2 and PuO_2 agglomerates, respectively, indicating similarity.

Figure 7 Mass concentration variation of PuO_2 aerosol with time in 17.4 liter chamber.

Figure 8 Mass concentration variation of PuO_2 aerosol with time in 0.75 m^3 chamber.

Figure 9a, 9b, 9c Comparison of PuO_2 size distribution at 10 min, 1 hr, and 7 hr

Figure 10 Variation of Count Median Diameter with time for Na- PuO_2 aerosol.

Figure 11 Mass concentration variation of Na- PuO_2 aerosol with time in 0.75 m^3 chamber

Figure 12 Cubic PuO_2 aerosol particles with NaOH spheres.

Figure 13 Variation of Count Median Diameter with time for UO_2 aerosol in 70% relative humidity.

Figure 14 Typical spherical UO_2 agglomerates in 70% relative humidity.

Figure 15 Particle size distribution of UO_2 aerosol in 70% relative humidity at 5 hr and 18 min.

Figure 16 Particle size distribution of UO_2 aerosol in 70% relative humidity at 28 hr and 18 min

Figure 17 a and 17b Particle size distribution of Na-UO₂ aerosol in 70% relative humidity at 5 hr and 18 min and 28 hr and 18 min, respectively.

Figure 18 Combined Na-UO₂ particles produced in 70% relative humidity.

Figure 19 Behavior of pure PuO₂ aerosols and mixed PuO₂-UO₂ aerosol.

Figure 20 Behavior of mixed PuO₂-Na aerosols.